



HAL
open science

Maintaining forest cover to enhance temperature buffering under future climate change

Emiel de Lombaerde, Pieter Vangansbeke, Jonathan Roger Michel Henri Lenoir, Koenraad van Meerbeek, Jonas Lembrechts, Francisco Rodríguez-Sánchez, Miska Luoto, Brett Scheffers, Stef Haesen, Juha Aalto, et al.

► To cite this version:

Emiel de Lombaerde, Pieter Vangansbeke, Jonathan Roger Michel Henri Lenoir, Koenraad van Meerbeek, Jonas Lembrechts, et al.. Maintaining forest cover to enhance temperature buffering under future climate change. *Science of the Total Environment*, 2022, 810 (151338), 10.1016/j.scitotenv.2021.151338 . hal-03624480

HAL Id: hal-03624480

<https://hal.inrae.fr/hal-03624480v1>

Submitted on 13 May 2022

HAL is a multi-disciplinary open access archive for the deposit and dissemination of scientific research documents, whether they are published or not. The documents may come from teaching and research institutions in France or abroad, or from public or private research centers.

L'archive ouverte pluridisciplinaire **HAL**, est destinée au dépôt et à la diffusion de documents scientifiques de niveau recherche, publiés ou non, émanant des établissements d'enseignement et de recherche français ou étrangers, des laboratoires publics ou privés.

1 **Maintaining forest cover to enhance temperature buffering under future climate**
2 **change**

3

4 Emiel DeLombaerde^a, Pieter Vangansbeke^a, Jonathan Lenoir^b, Koenraad Van Meerbeek^c, Jonas Lembrechts^d,
5 Francisco Rodríguez-Sánchez^e, Miska Luoto^f, Brett Scheffers^g, Stef Haesen^c, Juha Aalto^h, Ditte Marie
6 Christiansenⁱ, Karen De Pauw^a, Leen Depauw^a, Sanne Govaert^a, Caroline Greiser^j, Arndt Hampe^j, Kristoffer
7 Hylander^k, David Klinges^l, Irena Koelemeijerⁱ, Camille Meeussen^a, Jerome Ogée^m, Pieter Sanczuk^a, Thomas
8 Vanneste^a, Florian Zellwegerⁿ, Lander Baeten^a, Pieter De Frenne^a

9

10 ^aForest and Nature Lab, Ghent University, Gontrode, Belgium

11 ^bEcologie et dynamique des systèmes anthropisés (EDYSAN), UMR CNRS 7058, Amiens, France

12 ^cDepartment of Earth and Environmental Sciences, KU Leuven, Leuven, Belgium

13 ^dResearch Group Plants and Ecosystems, University of Antwerp, Wilrijk, Belgium

14 ^eDept. Biología Vegetal y Ecología, Universidad de Sevilla, Sevilla, Spain

15 ^fDepartment of Geosciences and Geography, University of Helsinki, Helsinki, Finland

16 ^gDepartment of Wildlife Ecology and Conservation, University of Florida, Gainesville, United States

17 ^hWeather and Climate Change Impact Research, Finnish Meteorological Institute, Helsinki, Finland

18 ⁱDepartment of Ecology, Environment and Plant Sciences, Stockholm University, Stockholm, Sweden

19 ^jBIOGECO, INRAE, Univ. Bordeaux, Cestas, France

20 ^kDepartment of Ecology, Environment and Plant Sciences, Bolin Centre for Climate Research, Stockholm
21 University, Stockholm, Sweden

22 ^lSchool of Natural Resources and Environment, University of Florida, Gainesville, United States

23 ^mINRAE, Bordeaux Science Agro, ISPA, Villenave d'Ornon, France

24 "Swiss Federal Institute for Forest, Snow and Landscape Research WSL, Birmensdorf, Switzerland

25

26 **Abstract**

27 Forest canopies buffer macroclimatic temperature fluctuations. However, we do not know if and how the
28 capacity of canopies to buffer understorey temperature will change with accelerating climate change. Here
29 we map the difference (offset) between temperatures inside and outside forests in the recent past and
30 project these into the future in boreal, temperate and tropical forests. Using linear mixed-effect models, we
31 combined a global database of 714 paired time series of temperatures (mean, minimum and maximum)
32 measured inside forests vs. in nearby open habitats with maps of macroclimate, topography and forest cover
33 to hindcast past (1970-2000) and to project future (2060-2080) temperature differences between free-air
34 temperatures and sub-canopy microclimates. For all tested future climate scenarios, we project that the
35 difference between maximum temperatures inside and outside forests across the globe will increase (i.e.
36 result in stronger cooling in forests), on average during 2060-2080, by 0.27 ± 0.16 °C (RCP2.6) and 0.60 ± 0.14
37 °C (RCP8.5) due to macroclimate changes. This suggests that extremely hot temperatures under forest
38 canopies will, on average, warm less than outside forests as macroclimate warms. This knowledge is of
39 utmost importance as it suggests that forest microclimates will warm at a slower rate than non-forested
40 areas, assuming that forest cover is maintained. Species adapted to colder growing conditions may thus find
41 shelter and survive longer than anticipated at a given forest site. This highlights the potential role of forests
42 as a whole as microrefugia for biodiversity under future climate change.

43 **Keywords:** forest microclimate, temperature offsets, canopy, climate change, future

44 climate projections, paired sensor data

45

46 **Introduction**

47 Warming temperatures and changing precipitation regimes are influencing ecosystems across the globe
48 (IPCC, 2018). To date, ecological research assessing the impact of anthropogenic climate change has
49 predominantly relied on macroclimatic data. These data are typically based on a global network of weather
50 stations established at approximately 1.5 to 2.0 m above the soil surface in open habitats (e.g. above short
51 grass) (World Meteorological Organization, 2018). Forest organisms living below and within tree canopies,
52 however, experience microclimatic conditions distinct from those in open habitats (Chen et al., 1999; De
53 Frenne et al., 2021; Geiger et al., 2009). Below tree canopies, lower radiation, wind and evapotranspiration
54 rates often translate into lower temporal variation in air temperature and humidity compared to open
55 environments (Davis et al., 2019; Geiger et al., 2009; Von Arx et al., 2013). In particular, temperature
56 extremes are often strongly attenuated in forest interiors, with lower maxima and higher minima compared
57 to open environments (De Frenne et al., 2019; Li et al., 2015). Studies have already shown that such
58 microclimatic buffering can mediate the response of forest communities to climate change (De Frenne et al.,
59 2013; Dietz et al., 2020; Lenoir et al., 2017; Stevens et al., 2015; Zellweger et al., 2020). Despite the increasing
60 evidence that ecosystem dynamics and processes are more likely to be related to forest microclimates than
61 to macroclimate (Chen et al., 2018; De Frenne et al., 2021; De Smedt et al., 2021; Frey et al., 2016a),
62 microclimates are still seldom incorporated in ecological research (e.g. in species distribution models)
63 (Lembrechts et al., 2019) and ignored by dynamic global vegetation models (DGVMs; e.g. Thrippleton,
64 Bugmann, Kramer-Priewasser, & Snell, 2016) that simulate the effects of future climate change on natural
65 vegetation and its carbon and water cycles. In particular, we do not know how forest microclimates will
66 change in the future as macroclimate changes (Lembrechts and Nijs, 2020).

67 Advances in studies on the effects of climate change on different organisms living below or in forest canopies
68 have often been limited by the availability of suitable microclimatic data (De Frenne et al., 2021). One robust
69 way to study forest microclimates is to use microclimate measurements from paired (inside vs. outside
70 forests) sensor networks to calculate temperature offsets, i.e. the absolute and instantaneous difference
71 between temperature inside (i.e., microclimate) and free-air temperatures outside forests (i.e.,

72 macroclimate) (*sensu* De Frenne et al., 2021). Negative offset values thus reflect cooler and positive offsets
73 warmer forest temperatures compared to outside forests. These empirical offset values for temperature can
74 be related to readily available environmental data using statistical modelling approaches, and these models
75 can then be used to interpolate and extrapolate microclimate across entire mapped landscapes (Frey et al.,
76 2016b; Greiser et al., 2018). Differences between macro- and microclimate (i.e., temperature offsets) result
77 from processes operating at many scales that influence incoming solar radiation, air mixing, soil properties
78 or evapotranspiration (reviewed in De Frenne et al., 2021). Macroclimatic conditions (e.g., mean temperature
79 and rainfall), topographic variation in the landscape (e.g., elevation and aspect) and variation in canopy cover
80 and vegetation height have been reported to be the main drivers of the understory temperatures in forests
81 (De Frenne et al., 2021, 2019; Greiser et al., 2018; Macek et al., 2019; Zellweger et al., 2019). With the advent
82 of global forest microclimate data (De Frenne et al., 2019; Zellweger et al., 2020), this type of modelling now
83 enables the prediction of forest microclimates across forest types under future climate change.

84 Here we map forest microclimate temperature offsets based on (i) paired sensor measurements below the
85 canopy vs. the open-air temperature at a given site and (ii) landscape- and canopy-scale predictors
86 throughout the year for the Earth's dominant forested ecosystems across five continents and at a spatial
87 resolution of ~1 km. More specifically, our objectives were to (1) make predictions for mean, minimum and
88 maximum temperatures using past macroclimatic data (1970-2000), and, (2) make projections for
89 temperature offsets for the future (2060-2080) macroclimatic conditions. We hypothesised that the
90 buffering capacity of forest canopies results in slower future warming of forest below-canopy temperatures
91 compared to the warming observed in standard meteorological weather stations (macroclimate).

92

93 **Material & Methods**

94 **Paired plot data**

95 We used a unique data set with 714 temperature offset data points involving paired plots from 74 studies
96 spread across 5 continents (Supplementary Material Fig. S1; Data available in De Frenne et al., 2019). Focus
97 was on air temperature below tree canopies (~72% of observations) and the temperature of the topsoil
98 (~28%), given their importance for responses of forest organisms and ecosystem functioning to macroclimate
99 warming. A key asset of this database is the paired nature of the data, which always combines below-canopy
100 temperature data at a given forest site with open-air temperature data from a neighbouring reference non-
101 forest site. Temperature measurement were performed by various logger types such as HOBO loggers (~15%
102 of observations), iButton loggers (~10%), full weather stations (~5%) and various other logger types (e.g.
103 cylindrical thermistor, Hanna thermohygrometer, thermocouples, etc.; ~70%). Reference sites were a nearby
104 open site equipped with the same type of (shielded) temperature loggers (~82% of observations), a nearby
105 weather station (~14%) (provided the distance did not conflict with the temperature offset of the canopy,
106 e.g., due to significant topographic differences) or a logger placed above the upper canopy surface (~4%). We
107 specifically refrained from using additional data on forest microclimate conditions that were not strictly
108 paired with free-air conditions from a neighbouring site using the exact same design (same sensor, same
109 logger, same shielding material, same height).

110 The data points were collated from the scientific literature in a systematic and reproducible manner (see De
111 Frenne et al., 2019 for full details). Temperature offsets were calculated as the temperature inside the forest
112 minus the temperature outside the forest, or extracted directly from the original study; negative values
113 reflect cooler temperatures below tree canopies while positive values reflect warmer understorey
114 temperatures. This was done for three temperature response variables, i.e. mean, maximum, and minimum
115 temperature (further referred to as T_{mean} , T_{min} and T_{max} , respectively) that were computed during a specific
116 time period that could differ between sites but that was exactly the same between paired sensors installed
117 outside and inside the forest at a given site. Multiple forest sites (at least several kilometres apart), seasons
118 (meteorological seasons, later aggregated to growing versus non-growing season) and temperature metrics

119 (maximum, mean, minimum, air or soil temperatures) originating from the same study were entered into
120 different rows of the database but tagged under the same study ID. Temperature values of long time series
121 were always aggregated per season and/or year, which means that several temperature values for T_{mean} , T_{min}
122 or T_{max} could be generated for the same study site. Temperature measurements were classified as having
123 taken place during the growing season, the non-growing season or throughout the whole year. This
124 classification was performed on the basis of reported meteorological seasons and/or climate information in
125 the original study. The dry and winter season were classified as the non-growing season in tropical and
126 temperate biomes, respectively. Estimates of uncertainty (standard error, standard deviation, coefficient of
127 variation or confidence intervals) of the temperature measurements were only reported for a small minority
128 (13.6%) of offset values in the database and were thus not included in our analyses. See De Frenne et al.
129 (2019) for more details on the literature search, inclusion criteria and the empirical data used in this study.

130 **Predictor variables**

131 To predict the offsets for the three temperature variables (T_{mean} , T_{max} , T_{min}) across all forests at a global extent,
132 we gathered global maps of predictor variables related to macroclimate, topography and forest cover. These
133 three sets of predictor variables were selected based on their importance for forest microclimate, and on the
134 spatial resolution and extent of the available data. All the predictor maps we used are raster maps with a
135 spatial resolution of 30 arcsec (~1 km) and are available at the global extent (i.e., from 80°N to 56°S in latitude
136 and from 180°E to 180°W in longitude). Values for all predictor variables were extracted using the
137 geographical coordinates for each plot pair.

138 *Macroclimate.* Global raster maps of mean, minimum and maximum free-air temperature (°C; T_{macro}),
139 on a monthly basis, as well as monthly precipitation (mm) raster maps, averaged for the climatology
140 1970-2000, were collected from WorldClim version 2.1 (Fick and Hijmans, 2017). In addition, we
141 gathered future projections (2060-2080) for the exact same set of temperature and precipitation
142 variables described in the previous sentence but based on the contrasting “very stringent”
143 representative concentration pathway (RCP) 2.6 and “worst case” RCP 8.5 from three different
144 general circulation models (GCMs) with minimal interdependency, based on Sanderson et al. (2015),

145 i.e. HadGEM2-ES, MPI-ESM-LR and MIROC5 (downscaled CMIP5 data from WorldClim; 30 arcsec
146 resolution).

147 *Topographic variables and distance to the coast.* We gathered six variables related to topography
148 using raster layers derived from the Global Multi-resolution Terrain Elevation Data 2010
149 (GMTED2010) dataset at 30 arcsec resolution (Amatulli et al., 2018). Maps on northness and
150 eastness, elevation (m a.s.l.), elevational variation (EleVar) and topographic position index (TPI) were
151 collected. Northness and eastness are the sine of the slope, multiplied by the cosine and sine of the
152 aspect, respectively. They provide continuous measures describing the orientation in combination
153 with the slope (i.e., a circular variable is transformed into a continuous one, ranging from -1 to 1). In
154 the Northern Hemisphere, a northness value close to 1 corresponds to a northern exposition on a
155 vertical slope (i.e., a slope exposed to very low amount of solar radiation), while a value close to -1
156 corresponds to a very steep southern slope, exposed to a high amount of solar radiation. Aspect
157 values for the Southern Hemisphere were inverted so that a value of 1 in the Southern Hemisphere
158 also means very low amount of solar radiation. Variables EleVar (1) and TPI (2) capture topographic
159 heterogeneity within a 1 km² grid cell around each pair of measurements (inside and outside forest):
160 (1) the standard deviation of elevational values aggregated per 1 km² grid cell (further referred to as
161 elevational variation) and (2) the median of the topographic position index (TPI) values across each
162 1 km² grid cell. The TPI is the difference between the elevation of a focal cell and the mean elevation
163 of its eight surrounding cells. Positive and negative values correspond to ridges and valleys,
164 respectively, while zero values correspond to flat areas (Amatulli et al., 2018). We also produced a
165 map with the distance from each land pixel to the nearest coastline (Dist2Coast) using the coastline
166 map data from Natural Earth (free vector data from naturalearthdata.com).

167 *Forest cover and forest height.* We used the tree canopy cover (defined as canopy closure for all
168 vegetation taller than 5 m in height) map for the year 2000 by Hansen et al. (2013). This high-
169 resolution global map layer was re-projected and aggregated from 30 m to 30 arcsec using the
170 average of the aggregated raster cells. This canopy cover map is the only available map spanning a
171 global extent at this high resolution. By using this data product, we make the strong assumption that

172 canopy cover at the time of temperature measurements is similar to the cover in the year 2000. We
173 consider this assumption as reasonable as the median year of the temperature measurements for all
174 data points is approximately 1996 (range between 1943 and 2014). Finally, we used estimates of
175 canopy height at 1 km resolution derived from the ICESat satellite mission based on 2005 (Simard et
176 al., 2011).

177 **Data analysis**

178 All statistical analyses were performed in the open-source statistical software environment of R, version 4.0.2
179 (R Core Team, 2021). The temperature offsets for T_{mean} , T_{max} and T_{min} were modelled (274, 184 and 202 plot
180 pairs respectively), after removing missing values for sensor height, i.e. not mentioned in the original study,
181 and data points with canopy cover zero (based on the tree canopy cover map introduced above; Hansen et
182 al., 2013) using linear mixed-effect models with random intercept (LMMs) (*lme4* package; Bates et al., 2015).
183 In our main models, we combined the seasonal (growing vs. non-growing and annual) time series and
184 performed additional analyses for the different three different time periods (see further and Supplementary
185 Material Appendix S2). We included 'study ID' as a random intercept term to account for non-independence
186 between samples within studies. For each of the three studied response variables, we started our modelling
187 protocol from the full model:

188 $T_{\text{offset}} \sim T_{\text{macro}} + \text{Precipitation} + \text{Elevation} + \text{Eastness} + \text{Northness} + \text{EleVar} + \text{TPI} + \text{Dist2Coast} + \text{Canopy cover} +$
189 $\text{Forest height} + \text{Sensor height} + \text{random effect 'study ID'}$

190 For T_{macro} , we used the monthly average for either T_{mean} , T_{max} and T_{min} temperature during the period 1970-
191 2000 depending on the studied response variable of T offset (T_{mean} , T_{max} or T_{min}). Sensor height was also
192 included in the models (continuous variable, in metres above or below the soil surface), as this significantly
193 impacts the magnitude of the temperature offset (De Frenne et al., 2019; Supplementary Fig. S2; Table S1).
194 Sensor height is positive for aboveground and negative for belowground sensors. Data points with sensor
195 height > 2 m were excluded as our aim was to model forest microclimate near the ground. To avoid
196 collinearity in predictor variables and improve model performance, we excluded variables that showed a
197 correlation $r \geq |0.7|$ (Pearson's product-moment correlation; Supplementary Fig. S3) and variance inflation

198 factor ≥ 4 (Zuur et al., 2010). Forest height was therefore removed from all models due to high correlation
199 with canopy cover; for T_{mean} offset, EleVar was also dropped from the model due to high correlation with TPI.
200 All predictors were standardized by subtracting the mean and dividing by the standard deviation prior to
201 modelling. For each response variable, the single best model was selected based on the Akaike Information
202 Criterion (AIC) using the automated dredge-function of the package MuMIn (Barton, 2009). Goodness of fit
203 was calculated following Nakagawa and Schielzeth (2013).

204 To test for non-linear relationships, we also used generalized additive mixed-effect models (GAMMs) (cf. the
205 *gam4* package) (Wood and Scheipl, 2014) on the same dataset. We applied smoothers to the same set of
206 fixed-effect terms, included the same random intercept term 'study ID' and followed the same model
207 selection procedure as for the LMMs. For each of the three studied response variables (T_{mean} , T_{max} , T_{min}) and
208 for each of the two modelling approaches, we performed a leave-one-out cross validation (LOOcv) and
209 compared root mean square errors (RMSE) among models (LMMs vs. GAMMs). We found no difference (t
210 test, p-value > 0.05) in RMSE between LMMs and GAMMs, justifying our choice of LMMs (see also
211 Supplementary Fig. S4). Furthermore, we checked spatial autocorrelation in the model residuals for the
212 LMMs using Moran's I-test from the *ape* package (Paradis and Schliep, 2019). No spatial autocorrelation was
213 detected (p-value > 0.05) in the model residuals. Additionally, we tested the effect of season of sampling
214 (annual, growing and non-growing season; see above) on each response variable. We included season as a
215 categorical variable to the full models described above and followed the same model selection procedure.
216 However, due to the low number of observations for each category (but growing season being the dominant
217 category), results including season were only included in the Supplementary Material Appendix S2.

218 Using the single best LMMs for each of our three response variables, we made predictions for T_{mean} , T_{max} , and
219 T_{min} offsets for forest across the globe using the collected map data for all predictor variables retained in the
220 models, setting sensor height to 1.0 m and not considering variation included in the random intercept.
221 Temperature offsets were predicted for all raster pixels (30 arcsec resolution) with canopy cover >50% as this
222 largely concurs with the global distribution of forest areas in the terrestrial ecoregions map by Olson et al.
223 (2001). To assess model performance, we performed spatially blocked k-fold cross-validation (k = 10; folds
224 assigned randomly, with spatial blocks of size 50 km²; Valavi et al., 2019). Furthermore, we made predictions

225 of future forest temperature offsets based on the future projections of temperature and precipitation (the
226 latter only included in the best model for T_{mean} and T_{min}) from WorldClim (see above). We made future
227 predictions for the period of 2060-2080 using the RCP 2.6 and RCP 8.5 projections based on the three selected
228 GCMs to account for uncertainty related to the GCMs; final model predictions for each RCP scenario were
229 averaged over all GCMs. For the future predictions, we assumed no change in topography and conservatively
230 assumed no change in canopy cover as our main goal was to determine direct climate change effects on
231 temperature offsets below forest canopies if we maintain the forest cover. Of course, we could use different
232 scenarios of future forest cover but we decided to not do that to better assess the unique effect of future
233 climate change without changing other parameters, such as forest cover, in the model. Besides, future
234 scenario on forest cover are not yet available at a global extent and at the spatial resolution we used here.
235 Uncertainty in predictions was mapped by applying a bootstrap approach. We resampled the original data
236 used to fit the models with replacement with total size of the bootstrap samples equal to the size of the
237 original sample. For each of the temperature responses, we fitted single best models using 30 bootstrap
238 samples. Using these 30 models, we generated per-pixel standard deviation mapped at the global extent
239 (Supplementary Fig. S5). To map uncertainty for the future predictions, the same procedure was followed for
240 each of the three GCMs, i.e. 30 bootstraps per GCM. Furthermore, we provide maps indicating where the
241 models are extrapolating beyond the values of data used to fit the models. Predictive performance and
242 uncertainty mapping were performed considering fixed effects of the models, excluding uncertainty of the
243 random (study) effects. Predictions were made using the *raster* package (Hijmans and van Etten, 2012).
244 Graphical plots were created using *ggplot2* (Wickham, 2016) and *Tmap* packages (Tennekes, 2018).

245 **Results**

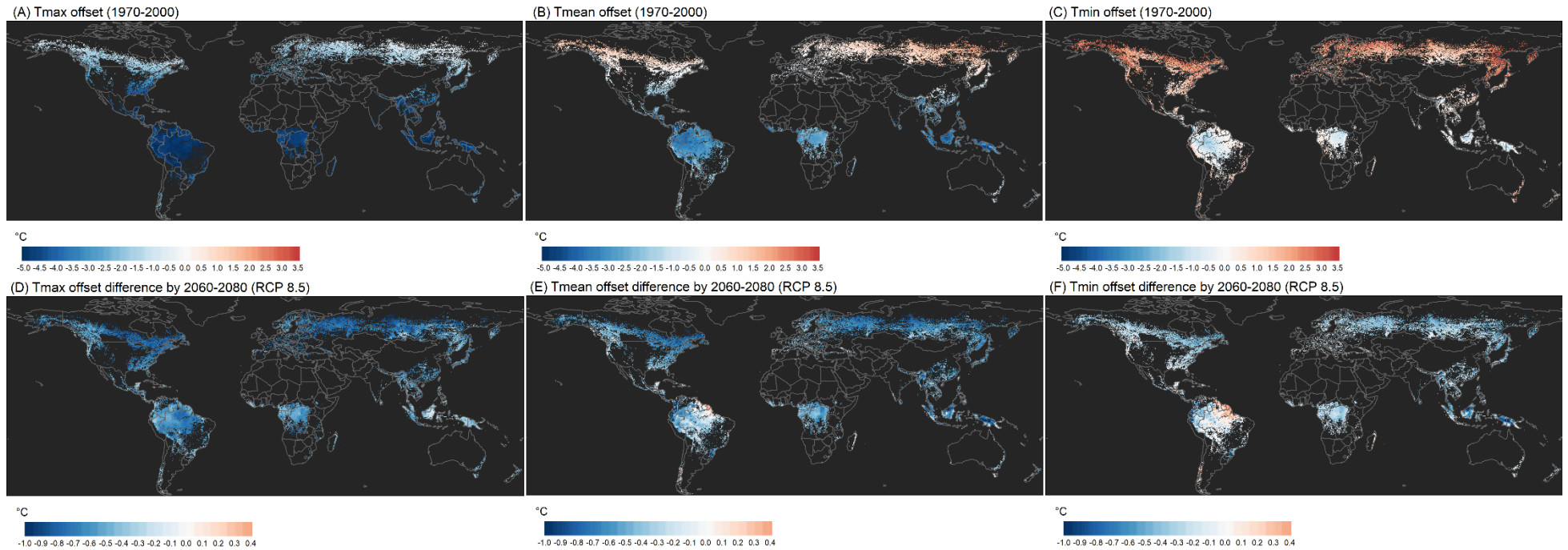
246 Our models predicted an average global offset of -2.92 ± 1.57 °C (mean \pm SD) for T_{max} , -0.88 ± 1.82 °C for T_{mean} ,
247 and 0.96 ± 1.27 °C for T_{min} (Fig. 1 and 2). These averages were calculated from all pixels having at least 50%
248 canopy cover during the year 2000 (Hansen et al., 2013) and derived from the predictions in Fig. 1. Our
249 predictions show a slightly positive T_{mean} offset (i.e. warmer temperatures within the forest) in boreal forests,
250 becoming overall negative towards the tropics (i.e. cooler temperatures within tropical forests compared to

251 free-air temperatures) (left panels Fig. 2). T_{\max} offsets are negative across the three biomes (i.e. cooler
252 maximum temperatures within forests) with the lowest values in the tropics (up to 5 degrees cooler within
253 forests), whereas T_{\min} offsets are positive in boreal and temperate forests and negative in the tropics (Fig. 2).
254 When including season in the modelling procedure, we found that for T_{mean} offsets were lower during the
255 growing season than for the non-growing season across the three biomes. For T_{\max} and T_{\min} , season was not
256 included in the best model (more detailed results included in Supplementary Material Appendix S2).

257 Offsets for T_{\max} , T_{mean} and T_{\min} were negatively affected by free-air, macroclimate temperatures
258 (Supplementary Fig. S2 and Table S1). For T_{mean} and T_{\min} , we found lower offset values with higher amounts
259 of precipitation (Supplementary Fig. S2 and Table S1), for T_{mean} this indicates stronger buffering (more
260 negative offsets), whereas for T_{\min} this means weaker buffering (offsets closer to zero). We found T_{\min} offsets
261 to be more positive, i.e. more strongly buffered, in areas with higher canopy cover, on pole-facing slopes and
262 closer to the coast. The marginal R^2 values (for fixed effects) were 0.29 (0.03 SD), 0.21 (0.03 SD) and 0.25
263 (0.03 SD), while conditional R^2 values (for fixed and random effects) reached 0.58 (0.04 SD), 0.60 (0.06 SD)
264 and 0.52 (0.04 SD) for T_{\max} , T_{mean} and T_{\min} , respectively. Root mean square errors obtained from the spatial
265 cross-validation were 3.67 °C (1.55 SD), 1.78 °C (0.71 SD) and 1.52 °C (0.45 SD) for T_{\max} , T_{mean} and T_{\min} ,
266 respectively. Standard deviations obtained from the bootstrapping procedure show fair consistency between
267 the predictions of the 30 bootstrapped models (Supplementary Table S2; Fig. S5 and S6). Upper confidence
268 levels (95%) of standard deviations for all three responses remained lower than 1 °C (Supplementary Table
269 S2 and Fig. S6). Higher values were mainly observed in the tropical and boreal region. We also found higher
270 extrapolation for the predictors included in the models in tropical forests and especially in the boreal region
271 (Supplementary Fig. S7).

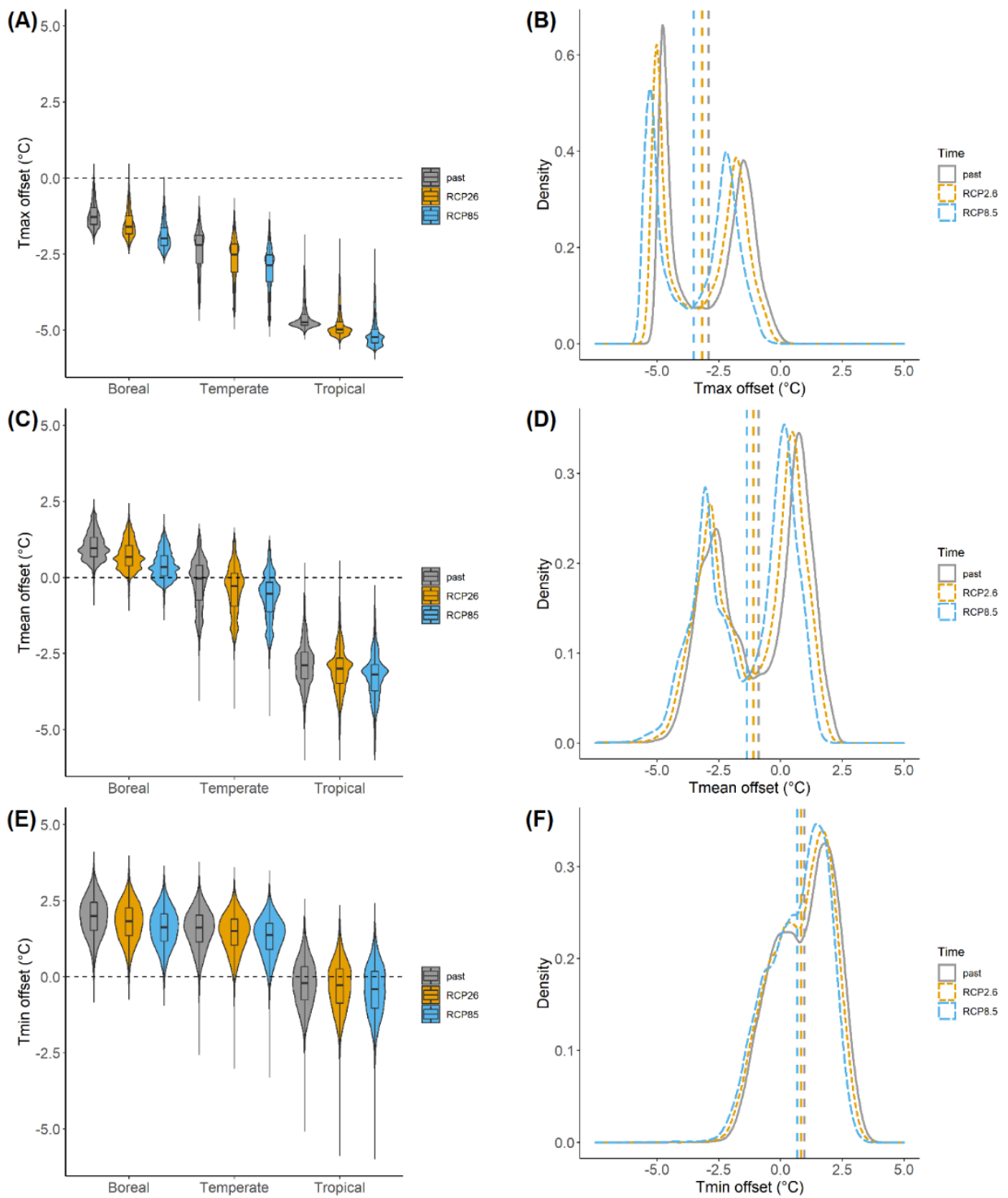
272 Our future projections showed an overall decrease in offset values for all three temperature responses (Fig.
273 2). For T_{mean} , future minus past offsets were -0.22 ± 0.16 °C (mean + SD) for RCP2.6 and -0.5 ± 0.22 °C for
274 RCP8.5 (Fig. 2). For T_{\max} , future minus past offsets were -0.27 ± 0.16 °C for RCP2.6 and -0.60 ± 0.14 °C for
275 RCP8.5 (i.e. cooler maximum temperatures within forests compared to outside temperatures in the future).
276 For T_{\min} , future minus past offsets were -0.12 ± 0.18 °C for RCP2.6 and -0.27 ± 0.24 °C for RCP8.5. These
277 averages were derived from panels D, E and F in Fig. 1. For both T_{\max} and T_{mean} , this means stronger offsets or

278 buffering (more negative offsets), whereas for T_{\min} weaker buffering (offsets closer to zero). Decreases in T_{\min}
279 offsets are most pronounced in the boreal and temperate region (left panels Fig. 2).



280

281 Fig. 1. First row: Global maps of past (1970-2000 climate) forest temperature offsets of (A) maximum, (B) mean and (C) minimum temperatures below tree canopies. Second row:
 282 Maps showing the difference between (D) maximum, (E) mean and (F) minimum temperature offset predictions based on future climatic conditions under RCP8.5 scenarios and past
 283 (1970-2000) offsets (future minus past, negative values thus depict lower offsets in the future than in the recent past which mean higher buffering for T_{max} and T_{mean} but lower for
 284 T_{min}). Predictions were made based on linear mixed-effects models and only for pixels where the canopy cover in the year 2000 is > 50% (Hansen et al., 2013).



285

286 Fig. 2. Left panels: Violin and box plots showing the distribution of predicted below-canopy forest temperature offsets
 287 of (A) T_{max} , (C) T_{mean} , and (E) T_{min} across boreal, temperate and tropical forests classified following Olson et al. (2001).
 288 Right panels: density plots for the predicted offsets of (B) T_{max} , (D) T_{mean} , and (F) T_{min} . Dashed vertical lines represent
 289 global mean offset values for the three temperature responses for past, and the future RCP2.6 and RCP8.5 scenarios.
 290 Note that bimodality is observed in the density plots, resulting from the difference between offsets in temperate and
 291 boreal versus tropical forests (see Fig. 1). For all plots, different colours and line types represent predictions for past
 292 climatic conditions (macroclimate temperature and precipitation, grey), for RCP2.6 (orange) and RCP8.5 scenarios
 293 (blue). Data points to draw these plots are subsamples (10^5 pixels) derived from the global predictions in Fig. 1.

294

295

296 Discussion

297 Our predictions of temperature offsets for the 1970-2000 climatology and for forests having at least 50% tree
298 cover during the year 2000 (Hansen et al., 2013) show that mean temperatures are on average cooler below
299 canopies (at 1 m height) than in open habitats across all forested grid cells (De Frenne et al., 2019; Li et al.,
300 2015). Our results also support the fact that temperature extremes are mainly buffered in forests; T_{\max} is on
301 average lower inside forests, whereas T_{\min} is warmer. Nevertheless, strong biome-specific variation was
302 observed: while in boreal forests, T_{mean} offsets were slightly positive, they became overall negative towards
303 the tropics. T_{\max} offsets were negative across the three biomes with the most negative values in the (warmer)
304 tropics, whereas T_{\min} offsets were positive in the cooler boreal and temperate forests, and negative in the
305 warm tropics. Furthermore, the difference between growing and non-growing season on T_{mean} offsets
306 illustrates the importance of considering the temporal and seasonal variation in temperature offsets in future
307 research (Li et al., 2015; Zellweger et al., 2019).

308 Temperature offsets for all three responses were negatively related to macroclimate temperatures. This
309 relationship is expected as temperature offsets are directly linked to macroclimate temperatures; if free-air
310 temperatures rise, offsets will become more negative because the parameter estimate for T_{macro} represents
311 the proportional buffering of canopies of free-air temperatures. Offsets for T_{mean} and T_{\min} were negatively
312 affected by precipitation. That is, the buffering for T_{\max} by canopies was stronger in regions with higher
313 amounts of precipitation, whereas buffering is lower for T_{\min} , supporting the notion that evapotranspiration
314 drives the offset in these conditions (Davis et al., 2019). The limited role of drivers other than macroclimate
315 could be because the 30 arcsec (~ 1 km) spatial resolution is still too coarse to detect effects of e.g. topography
316 or canopy cover, drivers acting on a very local scale (Ashcroft and Gollan, 2012; Greiser et al., 2018; Macek
317 et al., 2019).

318 Our aim was not to produce maps for use, but to give an overview of how temperature offsets between
319 forest and open habitats vary across forest biomes and how these relationships can evolve under climate
320 change. Despite the limitations of the data and the assumptions made, we found that our models explained
321 a moderately large amount of variation in the offsets, and considered model accuracy to be fair. Uncertainty

322 in predictions increased towards tropical and boreal forests which is likely caused by extrapolation outside
323 the environmental range included in our data. These biomes were underrepresented in the data, hence,
324 future research should focus on setting out networks of paired temperature sensors in these regions
325 (Lembrechts et al., 2021b).

326 Our projections for both the “very stringent” RCP2.6 as well as the “worst-case” RCP8.5 scenario indicate
327 that buffering by forest canopies for T_{mean} and T_{max} temperature may increase, but minimum temperature
328 offsets will decrease, especially in temperate and boreal regions as ambient temperatures become less cold.
329 This suggests that under climate change, free-air temperatures are likely to have a larger-magnitude increase
330 than the corresponding forest microclimate temperatures, which would reinforce the idea of divergent
331 warming (decoupling) between macroclimate and microclimate (De Frenne et al., 2019; Lenoir et al., 2017).
332 Offsets may even become lower (resulting in increasing or decreasing buffering for T_{mean} or T_{min} , respectively)
333 despite projected decreases in precipitation in some regions (Supplementary Fig. S8). It is possible that finer-
334 grained microclimatic heterogeneity could buffer the impact of a changing macroclimate even further
335 (Maclean et al., 2017). This inference relies, however, on the strong assumption that forest cover and
336 composition will remain stable in the future. Such stability is however unlikely, as climate change itself as
337 well as forest management and disturbances can either increase or decrease forest canopy cover in the
338 future. For example, climate change is however likely to cause increased tree mortality owing to, for instance,
339 repeated and more severe disturbances such as droughts, fires, pathogens and insect outbreaks (Curtis et
340 al., 2018; Senf et al., 2021; Senf and Seidl, 2020). The resulting reduction in tree canopy cover can lead to a
341 sudden loss (i.e. a tipping point) of canopy buffering and increased microclimate warming (Alkama and
342 Cescatti, 2016; Findell et al., 2017; Lembrechts and Nijs, 2020; Richard et al., 2021; Zellweger et al., 2020).
343 On the other hand, strong efforts are being made worldwide to increase forest cover and implement climate-
344 smart forestry practices (Bastin et al., 2019; Di Sacco et al., 2021). How these forest cover changes will affect
345 future forest temperature buffering should be a topic for future forest microclimate research.

346 We projected temperature buffering capacities of forests across the globe under future climate change
347 scenarios. Assuming no change in forest composition, we predicted that forest buffering of T_{mean} and T_{max} will
348 increase in the future (2060-2080), whereas buffering of T_{min} will be reduced due to changes in macroclimate

349 conditions. Our results indicate that the refugial capacity of cool and dense forest might last longer than
350 anticipated in a warming climate. This knowledge has important implications for forest biodiversity
351 conservation. Forest managers and policymakers could, for example, aim to optimise forest functioning and
352 biodiversity goals by identifying areas in which reducing or retaining canopy cover may have larger impacts
353 on the prevailing microclimate than anticipated under future climate change (Wolf et al., 2021). The paired
354 nature of the data allowed us to model absolute temperature offsets across a global extent with fair accuracy.
355 Gridded microclimate products such as ours, especially when paired with new, well-designed networks of
356 microclimate measurements (Lembrechts et al., 2020) serve ecological and environmental modelers with a
357 more scale-relevant set of products for making predictions and drawing inference. At the regional and even
358 continental scale, novel high-resolution data on forest structure and composition based on remote sensing
359 imagery (e.g. GEDI LiDAR data) are becoming available (De Frenne et al., 2021; Lembrechts et al., 2019;
360 Randin et al., 2020; Zellweger et al., 2018). Including these microclimate measurements and novel spatial
361 map data (e.g. Haesen et al., 2021; Lembrechts et al., 2020) in future models and mapping efforts will increase
362 accuracy of future predictions (Lembrechts et al., 2021a). Our study illustrates that forest microclimates
363 themselves are subject to climate change, which will have important consequences for forest-dwelling
364 species and must hence not be neglected.

365 **Data availability:**

366 The dataset analysed in the current study is available in the Figshare repository, with the identifier
367 10.6084/m9.figshare.7604849 (de Frenne et al., 2019).

368 **Acknowledgements:**

369 EDL, PV, PDF, LD, PS, CM and TV received funding from the European Research Council (ERC) under the
370 European Union's Horizon 2020 research and innovation programme (ERC Starting Grant FORMICA 757833).
371 FZ received funding from the Swiss National Science Foundation (grant number 193645). SH received funding
372 from a FLOF fellowship of the KU Leuven (project nr. 3E190655). Funding for DHK was provided by the
373 National Science Foundation Graduate Research Fellowship Program (DGE-1842473). JA acknowledges
374 Academy of Finland Flagship funding (grant no. 337552). KH received funding from the Swedish Research
375 Council Formas (grants 2014-530 and 2018-2829) and the Bolin Centre for Climate Research, Stockholm
376 University. SG was supported by the Research Foundation Flanders (FWO) (project G0H1517N). JLL received
377 funding from the Research Foundation Flanders (FWO) (project 12P1819N). JL received funding from the
378 Agence Nationale de la Recherche (ANR) within the framework of the IMPRINT project "IMpacts des

379 PProcessus microclimatiques sur la redistributioN de la biodiversité forestière en contexte de réchauffement
380 du macroclimat” (grant number: ANR-19-CE32-0005-01). KDP received funding from the Research
381 Foundation Flanders (FWO) (project ASP035-19). FRS was supported by the VI Plan Propio de Investigación
382 of Universidad de Sevilla (VI PPIT- US).

383

384

385 **References**

- 386 Alkama, R., Cescatti, A., 2016. Climate change: Biophysical climate impacts of recent changes in global
387 forest cover. *Science* (80-). 351, 600–604. <https://doi.org/10.1126/science.aac8083>
- 388 Amatulli, G., Domisch, S., Tuanmu, M.N., Parmentier, B., Ranipeta, A., Malczyk, J., Jetz, W., 2018. Data
389 Descriptor: A suite of global, cross-scale topographic variables for environmental and biodiversity
390 modeling. *Sci. Data* 5, 1–15. <https://doi.org/10.1038/sdata.2018.40>
- 391 Ashcroft, M.B., Gollan, J.R., 2012. Fine-resolution (25 m) topoclimatic grids of near-surface (5 cm) extreme
392 temperatures and humidities across various habitats in a large (200 × 300 km) and diverse region. *Int.*
393 *J. Climatol.* 32, 2134–2148. <https://doi.org/10.1002/joc.2428>
- 394 Barton, K., 2009. MuMIn: Multi-Model Inference.
- 395 Bastin, J., Finegold, Y., Garcia, C., Mollicone, D., Rezende, M., Routh, D., Zohner, C., Crowther, T., 2019. The
396 global tree restoration potential. *Science* (80-). 365, 76–79. <https://doi.org/10.1126/science.aay8060>
- 397 Bates, D., Maechler, M., Bolker, B.M., Walker, S., 2015. Fitting Linear Mixed-Effects Models Using lme4. *J.*
398 *Stat. Softw.* 67, 1–48. <https://doi.org/10.18637/jss.v067.i01>
- 399 Chen, J., Saunders, S.C., Crow, T.R., Naiman, R.J., Brosofske, K.D., Mroz, G.D., Brookshire, B.L., Franklin, J.F.,
400 1999. Microclimate in forest ecosystem and landscape ecology: Variations in local climate can be used
401 to monitor and compare the effects of different management regimes. *Bioscience* 49, 288–297.
402 <https://doi.org/10.2307/1313612>
- 403 Chen, Y., Liu, Y., Zhang, J., Yang, W., He, R., Deng, C., 2018. Microclimate exerts greater control over litter
404 decomposition and enzyme activity than litter quality in an alpine forest-tundra ecotone. *Sci. Rep.* 8,
405 1–13. <https://doi.org/10.1038/s41598-018-33186-4>
- 406 Curtis, P.G., Slay, C.M., Harris, N.L., Tyukavina, A., Hansen, M.C., 2018. Classifying drivers of global forest
407 loss. *Science* (80-). 361, 1108–1111. <https://doi.org/10.1126/science.aau3445>
- 408 Davis, K.T., Dobrowski, S.Z., Holden, Z.A., Higuera, P.E., Abatzoglou, J.T., 2019. Microclimatic buffering in
409 forests of the future: the role of local water balance. *Ecography* (Cop.). 42, 1–11.
410 <https://doi.org/10.1111/ecog.03836>
- 411 De Frenne, P., Lenoir, J., Luoto, M., Scheffers, B.R., Zellweger, F., Aalto, J., Ashcroft, M.B., Christiansen,
412 D.M., Decocq, G., Pauw, K. De, Govaert, S., Greiser, C., Gril, E., Hampe, A., Jucker, T., Klinges, D.H.,
413 Koelemeijer, I.A., Lembrechts, J.J., Marrec, R., Meeussen, C., Ogée, J., Tyystjärvi, V., Vangansbeke, P.,
414 Hylander, K., 2021. Forest microclimates and climate change : Importance, drivers and future research
415 agenda. *Glob. Chang. Biol.* 1–19. <https://doi.org/10.1111/gcb.15569>
- 416 de Frenne, P., Lenoir, J., Rodriguez-Sanchez, F., 2019. Global buffering of temperatures under forest
417 canopies data and code. Figshare. <https://doi.org/10.6084/m9.figshare.7604849tem>
- 418 De Frenne, P., Rodríguez-Sánchez, F., Coomes, D.A., Baeten, L., Verstraeten, G., Vellend, M., Bernhardt-
419 Römermann, M., Brown, C.D., Brunet, J., Cornelis, J., Decocq, G.M., Dierschke, H., Eriksson, O., Gilliam,
420 F.S., Hédli, R., Heinken, T., Hermy, M., Hommel, P., Jenkins, M. a, Kelly, D.L., Kirby, K.J., Mitchell, F.J.G.,
421 Naaf, T., Newman, M., Peterken, G., Petřík, P., Schultz, J., Sonnier, G., Van Calster, H., Waller, D.M.,
422 Walther, G.-R., White, P.S., Woods, K.D., Wulf, M., Graae, B.J., Verheyen, K., 2013. Microclimate
423 moderates plant responses to macroclimate warming. *Proc. Natl. Acad. Sci. U. S. A.* 110, 18561–
424 18565. <https://doi.org/10.1073/pnas.1311190110>
- 425 De Frenne, P., Zellweger, F., Rodríguez-Sánchez, F., Scheffers, B.R., Hylander, K., Luoto, M., Vellend, M.,
426 Verheyen, K., Lenoir, J., 2019. Global buffering of temperatures under forest canopies. *Nat. Ecol. Evol.*
427 3, 744–749. <https://doi.org/10.1038/s41559-019-0842-1>
- 428 De Smedt, P., Boeraeve, P., Baeten, L., 2021. Intra-annual activity patterns of terrestrial isopods are

- 429 tempered in forest compared to open habitat. *Soil Biol. Biochem.* 160, 108342.
430 <https://doi.org/10.1016/j.soilbio.2021.108342>
- 431 Di Sacco, A., Hardwick, K.A., Blakesley, D., Brancalion, P.H.S., Breman, E., Cecilio Rebola, L., Chomba, S.,
432 Dixon, K., Elliott, S., Ruyonga, G., Shaw, K., Smith, P., Smith, R.J., Antonelli, A., 2021. Ten golden rules
433 for reforestation to optimize carbon sequestration, biodiversity recovery and livelihood benefits. *Glob.*
434 *Chang. Biol.* 27, 1328–1348. <https://doi.org/10.1111/gcb.15498>
- 435 Dietz, L., Collet, C., Dupouey, J.L., Lacombe, E., Laurent, L., Gégout, J.C., 2020. Windstorm-induced canopy
436 openings accelerate temperate forest adaptation to global warming. *Glob. Ecol. Biogeogr.* 2067–2077.
437 <https://doi.org/10.1111/geb.13177>
- 438 Fick, S.E., Hijmans, R.J., 2017. WorldClim 2: new 1-km spatial resolution climate surfaces for global land
439 areas. *Int. J. Climatol.* 37, 4302–4315. <https://doi.org/10.1002/joc.5086>
- 440 Findell, K.L., Berg, A., Gentine, P., Krasting, J.P., Lintner, B.R., Malyshev, S., Santanello, J.A., Shevliakova, E.,
441 2017. The impact of anthropogenic land use and land cover change on regional climate extremes. *Nat.*
442 *Commun.* 8, 1–9. <https://doi.org/10.1038/s41467-017-01038-w>
- 443 Frey, S.J.K., Hadley, A.S., Betts, M.G., 2016a. Microclimate predicts within-season distribution dynamics of
444 montane forest birds. *Divers. Distrib.* 22, 944–959. <https://doi.org/10.1111/ddi.12456>
- 445 Frey, S.J.K., Hadley, A.S., Johnson, S.L., Schulze, M., Jones, J.A., Betts, M.G., 2016b. Spatial models reveal the
446 microclimatic buffering capacity of old-growth forests. *Sci. Adv.* 2.
447 <https://doi.org/10.1126/sciadv.1501392>
- 448 Geiger, R., Aron, R., Todhunter, P., 2009. *The climate near the ground.* Rowman & Littlefield.
- 449 Greiser, C., Meineri, E., Luoto, M., Ehrlén, J., Hylander, K., 2018. Monthly microclimate models in a
450 managed boreal forest landscape. *Agric. For. Meteorol.* 250–251, 147–158.
451 <https://doi.org/10.1016/j.agrformet.2017.12.252>
- 452 Haesen, S., Lembrechts, J.J., De Frenne, P., Lenoir, J., Aalto, J., Ashcroft, M.B., Kopecký, M., Luoto, M.,
453 Maclean, I., Nijs, I., Niittynen, P., Hoogen, J., Arriga, N., Brůna, J., Buchmann, N., Čiliak, M., Collalti, A.,
454 De Lombaerde, E., Descombes, P., Gharun, M., Goded, I., Govaert, S., Greiser, C., Grelle, A., Gruening,
455 C., Hederová, L., Hylander, K., Kreyling, J., Kruijt, B., Macek, M., Máliš, F., Man, M., Manca, G., Matula,
456 R., Meeussen, C., Merinero, S., Minerbi, S., Montagnani, L., Muffler, L., Ogaya, R., Penuelas, J., Plichta,
457 R., Portillo-Estrada, M., Schmeddes, J., Shekhar, A., Spicher, F., Ujházyová, M., Vangansbeke, P.,
458 Weigel, R., Wild, J., Zellweger, F., Van Meerbeek, K., 2021. ForestTemp – Sub-canopy microclimate
459 temperatures of European forests. *Glob. Chang. Biol.* 1–13. <https://doi.org/10.1111/gcb.15892>
- 460 Hansen, M.C., Potapov, P. V., Moore, R., Hancher, M., Turubanova, S.A., Tyukavina, A., Thau, D., Stehman, S.
461 V, Goetz, S.J., Loveland, T.R., Kommareddy, A., Egorov, A., Chini, L., Justice, C.O., Townshend, J.R.G.,
462 2013. High-Resolution Global Maps of 21st-Century Forest Cover Change. *Science (80-)*. 342, 850–
463 854. <https://doi.org/10.1126/science.1244693>
- 464 Hijmans, R.J., van Etten, J., 2012. *raster: Geographic analysis and modeling with raster data.*
- 465 IPCC, 2018. *Global Warming of 1.5 °C - SR15 - Summary for Policy Makers, IPCC Climate Change Synthesis*
466 *Report.*
- 467 Lembrechts, J.J., Aalto, J., Ashcroft, M.B., De Frenne, P., Kopecký, M., Lenoir, J., Luoto, M., Maclean, I.M.D.,
468 Roupsard, O., Fuentes-Lillo, E., García, R.A., Pellissier, L., Pitteloud, C., Alatalo, J.M., Smith, S.W., Björk,
469 R.G., Muffler, L., Ratier Backes, A., Cesarz, S., Gottschall, F., Okello, J., Urban, J., Plichta, R., Svátek, M.,
470 Phartyal, S.S., Wipf, S., Eisenhauer, N., Puşcaş, M., Turtureanu, P.D., Varlagin, A., Dimarco, R.D., Jump,
471 A.S., Randall, K., Dorrepaal, E., Larson, K., Walz, J., Vitale, L., Svoboda, M., Finger Higgens, R.,
472 Halbritter, A.H., Curasi, S.R., Klupar, I., Koontz, A., Pearce, W.D., Simpson, E., Stemkovski, M., Jessen
473 Graae, B., Vedel Sørensen, M., Høye, T.T., Fernández Calzado, M.R., Lorite, J., Carbognani, M.,
474 Tomaselli, M., Forte, T.G.W., Petraglia, A., Haesen, S., Somers, B., Van Meerbeek, K., Björkman, M.P.,

475 Hylander, K., Merinero, S., Gharun, M., Buchmann, N., Dolezal, J., Matula, R., Thomas, A.D., Bailey, J.J.,
476 Ghosn, D., Kazakis, G., de Pablo, M.A., Kemppinen, J., Niittynen, P., Rew, L., Seipel, T., Larson, C.,
477 Speed, J.D.M., Ardö, J., Cannone, N., Guglielmin, M., Malfasi, F., Bader, M.Y., Canessa, R., Stanisci, A.,
478 Kreyling, J., Schmeddes, J., Teuber, L., Aschero, V., Čiliak, M., Máliš, F., De Smedt, P., Govaert, S.,
479 Meeussen, C., Vangansbeke, P., Gigauri, K., Lamprecht, A., Pauli, H., Steinbauer, K., Winkler, M.,
480 Ueyama, M., Nuñez, M.A., Ursu, T.M., Haider, S., Wedegärtner, R.E.M., Smiljanic, M., Trouillier, M.,
481 Wilmking, M., Altman, J., Brůna, J., Hederová, L., Macek, M., Man, M., Wild, J., Vittoz, P., Pärtel, M.,
482 Barančok, P., Kanka, R., Kollár, J., Palaj, A., Barros, A., Mazzolari, A.C., Bauters, M., Boeckx, P., Benito
483 Alonso, J.L., Zong, S., Di Cecco, V., Sitková, Z., Tielbörger, K., van den Brink, L., Weigel, R., Homeier, J.,
484 Dahlberg, C.J., Medinets, S., Medinets, V., De Boeck, H.J., Portillo-Estrada, M., Verryckt, L.T., Milbau,
485 A., Daskalova, G.N., Thomas, H.J.D., Myers-Smith, I.H., Blonder, B., Stephan, J.G., Descombes, P.,
486 Zellweger, F., Frei, E.R., Heinesch, B., Andrews, C., Dick, J., Siebicke, L., Rocha, A., Senior, R.A., Rixen,
487 C., Jimenez, J.J., Boike, J., Pauchard, A., Scholten, T., Scheffers, B., Klinges, D., Basham, E.W., Zhang, J.,
488 Zhang, Z., Géron, C., Fazlioglu, F., Candan, O., Sallo Bravo, J., Hrbacek, F., Laska, K., Cremonese, E.,
489 Haase, P., Moyano, F.E., Rossi, C., Nijs, I., 2020. SoilTemp: A global database of near-surface
490 temperature. *Glob. Chang. Biol.* 26, 6616–6629. <https://doi.org/10.1111/gcb.15123>

491 Lembrechts, J.J., Hoogen, J. Van Den, Aalto, J., Ashcroft, M.B., De Frenne, P., Kemppinen, J., Kopecký, M.,
492 2021a. Mismatches between soil and air temperature. *EcoEvoRxiv*.
493 <https://doi.org/10.32942/osf.io/pksqw>

494 Lembrechts, J.J., Lenoir, J., Frenne, P. De, Scheffers, B.R., 2021b. Designing countrywide and regional
495 microclimate networks 1–7. <https://doi.org/10.1111/geb.13290>

496 Lembrechts, J.J., Nijs, I., 2020. Microclimate shifts in a d ynamic world. *Science* (80-). 368, 711–712.

497 Lembrechts, J.J., Nijs, I., Lenoir, J., 2019. Incorporating microclimate into species distribution models.
498 *Ecography (Cop.)*. 42, 1267–1279. <https://doi.org/10.1111/ecog.03947>

499 Lenoir, J., Hattab, T., Pierre, G., 2017. Climatic microrefugia under anthropogenic climate change:
500 implications for species redistribution. *Ecography (Cop.)*. 40, 253–266.
501 <https://doi.org/10.1111/ecog.02788>

502 Li, Y., Zhao, M., Motesharrei, S., Mu, Q., Kalnay, E., Li, S., 2015. Local cooling and warming effects of forests
503 based on satellite observations. *Nat. Commun.* 6. <https://doi.org/10.1038/ncomms7603>

504 Macek, M., Kopecký, M., Wild, J., 2019. Maximum air temperature controlled by landscape topography
505 affects plant species composition in temperate forests. *Landsc. Ecol.* 34, 2541–2556.
506 <https://doi.org/10.1007/s10980-019-00903-x>

507 Maclean, I.M.D., Suggitt, A.J., Wilson, R.J., Duffy, J.P., Bennie, J.J., 2017. Fine-scale climate change:
508 modelling spatial variation in biologically meaningful rates of warming. *Glob. Chang. Biol.* 23, 256–
509 268. <https://doi.org/10.1111/gcb.13343>

510 Nakagawa, S., Schielzeth, H., 2013. A general and simple method for obtaining R² from generalized linear
511 mixed-effects models. *Methods Ecol. Evol.* 4, 133–142. <https://doi.org/10.1111/j.2041->
512 [210x.2012.00261.x](https://doi.org/10.1111/j.2041-210x.2012.00261.x)

513 Olson, D.M., Dinerstein, E., Wikramanayake, E.D., Burgess, N.D., Powell, G.V.N., Underwood, E.C., Amico,
514 J.A.D., Itoua, I., Strand, H.E., Morrison, J.C., Loucks, J., Allnutt, T.F., Ricketts, T.H., Kura, Y., Lamoreux,
515 J.F., Wesley, W., Hedao, P., Kassem, K.R., 2001. *Terrestrial Ecoregions of the World : A New Map of*
516 *Life on Earth* 51, 933–938.

517 Paradis, E., Schliep, K., 2019. Ape 5.0: An environment for modern phylogenetics and evolutionary analyses
518 in R. *Bioinformatics* 35, 526–528. <https://doi.org/10.1093/bioinformatics/bty633>

519 R Core Team, 2021. R: A language and environment for statistical computing.

520 Randin, C.F., Ashcroft, M.B., Bolliger, J., Cavender-Bares, J., Coops, N.C., Dullinger, S., Dirnböck, T., Eckert,

- 521 S., Ellis, E., Fernández, N., Giuliani, G., Guisan, A., Jetz, W., Joost, S., Karger, D., Lembrechts, J., Lenoir,
522 J., Luoto, M., Morin, X., Price, B., Rocchini, D., Schaeppman, M., Schmid, B., Verburg, P., Wilson, A.,
523 Woodcock, P., Yoccoz, N., Payne, D., 2020. Monitoring biodiversity in the Anthropocene using remote
524 sensing in species distribution models. *Remote Sens. Environ.* 239, 111626.
525 <https://doi.org/10.1016/j.rse.2019.111626>
- 526 Richard, B., Dupouey, J.L., Corcket, E., Alard, D., Archaux, F., Aubert, M., Boulanger, V., Gillet, F., Langlois, E.,
527 Macé, S., Montpied, P., Beaufils, T., Begeot, C., Behr, P., Boissier, J.M., Camaret, S., Chevalier, R.,
528 Decocq, G., Dumas, Y., Eynard-Machet, R., Gégout, J.C., Huet, S., Malécot, V., Margerie, P., Mouly, A.,
529 Paul, T., Renaux, B., Ruffaldi, P., Spicher, F., Thirion, E., Ulrich, E., Nicolas, M., Lenoir, J., 2021. The
530 climatic debt is growing in the understorey of temperate forests: Stand characteristics matter. *Glob.
531 Ecol. Biogeogr.* 30, 1474–1487. <https://doi.org/10.1111/geb.13312>
- 532 Sanderson, B.M., Knutti, R., Caldwell, P., 2015. A representative democracy to reduce interdependency in a
533 multimodel ensemble. *J. Clim.* 28, 5171–5194. <https://doi.org/10.1175/JCLI-D-14-00362.1>
- 534 Senf, C., Sebal, J., Seidl, R., 2021. Increasing canopy mortality affects the future demographic structure of
535 Europe's forests. *One Earth* 1–7. <https://doi.org/10.1016/j.oneear.2021.04.008>
- 536 Senf, C., Seidl, R., 2020. Mapping the forest disturbance regimes of Europe. *Nat. Sustain.*
537 <https://doi.org/10.1038/s41893-020-00609-y>
- 538 Simard, M., Pinto, N., Fisher, J.B., Baccini, A., 2011. Mapping forest canopy height globally with spaceborne
539 lidar. *J. Geophys. Res. Biogeosciences* 116, 1–12. <https://doi.org/10.1029/2011JG001708>
- 540 Stevens, J.T., Safford, H.D., Harrison, S., Latimer, A.M., 2015. Forest disturbance accelerates
541 thermophilization of understory plant communities. *J. Ecol.* 103, 1253–1263.
542 <https://doi.org/10.1111/1365-2745.12426>
- 543 Tennekes, M., 2018. Tmap: Thematic maps in R. *J. Stat. Softw.* 84. <https://doi.org/10.18637/jss.v084.i06>
- 544 Thrippleton, T., Bugmann, H., Kramer-Priewasser, K., Snell, R.S., 2016. Herbaceous Understorey : An
545 Overlooked Player in Forest Landscape Dynamics? *Ecosystems* 19, 1240–1254.
546 <https://doi.org/10.1007/s10021-016-9999-5>
- 547 Valavi, R., Elith, J., Lahoz-Monfort, J.J., Guillera-Arroita, G., 2019. blockCV: An r package for generating
548 spatially or environmentally separated folds for k-fold cross-validation of species distribution models.
549 *Methods Ecol. Evol.* 10, 225–232. <https://doi.org/10.1111/2041-210X.13107>
- 550 Von Arx, G., Graf Pannatier, E., Thimonier, A., Rebetez, M., 2013. Microclimate in forests with varying leaf
551 area index and soil moisture: Potential implications for seedling establishment in a changing climate. *J.
552 Ecol.* 101, 1201–1213. <https://doi.org/10.1111/1365-2745.12121>
- 553 Wickham, H., 2016. *ggplot2: elegant graphics for data analysis*. Springer, New York, USA.
- 554 Wolf, C., Bell, D.M., Kim, H., Paul, M., Schulze, M., Betts, M.G., Northwest, P., Service, U.F., Way, S.W.J., Or,
555 C., 2021. Temporal consistency of undercanopy thermal refugia in old-growth forest. *Agric. For.
556 Meteorol.* 307, 108520. <https://doi.org/10.1016/j.agrformet.2021.108520>
- 557 Wood, S., Scheipl, F., 2014. *gamm4: Generalized additive mixed models using mgcv and lme4*.
- 558 World Meteorological Organization, 2018. *Guide to meteorological instruments and methods of
559 observation, 2018 Editi. ed. WMO*.
- 560 Zellweger, F., Coomes, D., Lenoir, J., Depauw, L., Maes, S.L., Wulf, M., Kirby, K.J., Brunet, J., Kopecký, M.,
561 Máliš, F., Schmidt, W., Heinrichs, S., den Ouden, J., Jaroszewicz, B., Buyse, G., Spicher, F., Verheyen, K.,
562 De Frenne, P., 2019. Seasonal drivers of understorey temperature buffering in temperate deciduous
563 forests across Europe. *Glob. Ecol. Biogeogr.* 28, 1774–1786. <https://doi.org/10.1111/geb.12991>
- 564 Zellweger, F., De Frenne, P., Lenoir, J., Rocchini, D., Coomes, D., 2018. Advances in microclimate ecology

565 arising from remote sensing. *Trends Ecol. Evol.* xx, 1–15. <https://doi.org/10.1016/j.tree.2018.12.012>

566 Zellweger, F., De Frenne, P., Lenoir, J., Vangansbeke, P., Verheyen, K., Bernhardt-römermann, M., Baeten,
567 L., Hédli, R., Berki, I., Brunet, J., Van Calster, H., Chudomelov, 2020. Forest microclimate dynamics drive
568 plant responses to warming. *Science* (80-.). 368, 772–775.

569 Zuur, A.F., Ieno, E.N., Elphick, C.S., 2010. A protocol for data exploration to avoid common statistical
570 problems 3–14. <https://doi.org/10.1111/j.2041-210X.2009.00001.x>

571